

Using magnetic hyperbolic metamaterials as high frequency tunable filters

Rair Macêdo, Karen L. Livesey, and Robert E. Camley

Citation: *Appl. Phys. Lett.* **113**, 121104 (2018); doi: 10.1063/1.5049602

View online: <https://doi.org/10.1063/1.5049602>

View Table of Contents: <http://aip.scitation.org/toc/apl/113/12>

Published by the [American Institute of Physics](#)

AIP | Conference Proceedings

**Get 30% off all
print proceedings!**

Enter Promotion Code **PDF30** at checkout



Using magnetic hyperbolic metamaterials as high frequency tunable filters

Rair Macêdo,^{1,a)} Karen L. Livesey,² and Robert E. Camley²

¹SUPA School of Physics and Astronomy, University of Glasgow, Glasgow G12 8QQ, United Kingdom

²Center for Magnetism and Magnetic Nanostructures, University of Colorado at Colorado Springs, Colorado Springs, Colorado 80918, USA

(Received 23 July 2018; accepted 2 September 2018; published online 18 September 2018)

Metamaterials have enabled a series of major advances in optical devices in the past decade. Here, we suggest a type of hyperbolic metamaterial based on spin canting in magnetic multi-layers. We show that these structures have unique features in microwave waveguides that act as tunable filters. In the resulting band pass filter, we demonstrate an exceptional frequency tunability of 30 GHz with external fields smaller than 500 Oe. Unlike single metallic ferromagnetic films, we also demonstrate a high-frequency band-stop filter at very low fields. *Published by AIP Publishing.*

<https://doi.org/10.1063/1.5049602>

Magnetic signal processing devices have been extensively investigated in the context of modern technologies including communication and radar systems.^{1–7} In order to improve the capabilities of devices operating at GHz frequencies, several magnetic media have been studied including Yttrium Iron Garnet (YIG),^{2,8–10} metallic ferromagnets,^{11–14} structured materials,^{15–19} and hexagonal ferrites.^{20–23} These are of particular interest as they are based on absorptions near ferromagnetic resonance frequencies, which can be tuned by externally applied magnetic fields.²⁴

One problem with current materials is that they generally require large magnetic fields to obtain higher operational frequencies.⁴ A number of solutions have been proposed to overcome this, including using structured ferromagnets to take advantage of shape anisotropy²⁵ or using materials, such as M-type barium hexagonal ferrites,²¹ with high magnetocrystalline anisotropy. However, both of these proposed solutions have additional issues. The structured ferromagnets tend to have wide absorption bands, while the hexagonal ferrites can be difficult to grow and often require high temperature processing steps. Plus, hexagonal ferrites require very large static applied magnetic fields to significantly tune the resonance frequency. Therefore, artificial structures have recently been suggested as a way to engineer these resonances at particular frequencies and with greater field-tunability.^{26–33}

In this letter, we explore the possibility of employing a simple thin-film magnetic metamaterial as a high frequency tunable filter. We investigate the behavior of a metamaterial composed of ferromagnetic layers that are antiferromagnetically coupled through spacer layers. Such a structure can have electromagnetic hyperbolic behavior similar to that of simple antiferromagnetic crystals but at lower frequencies.³⁴ As an example, we calculate the propagation of transverse magnetic (TM) waves through a microscopic waveguide containing a Co/Ru multilayer³⁵ and find that we can obtain an operational band-stop frequency of 40 GHz at zero applied field, with an attenuation close to 30 dB/cm. In addition, we show how these metamaterials can be employed as band pass filters, with significant frequency tunability, and

with a change in the operational frequency of 30 GHz with just a 0.45 kOe static applied field.

Antiferromagnets are of particular interest due to their tunable hyperbolic dispersion when an external magnetic field is applied perpendicular to the spin direction, resulting in a canted spin system.³⁶ Most natural antiferromagnets, however, have very high resonance frequencies (in the THz range) and are difficult to tune because of large anisotropy.^{37–39} In the layered metamaterial system, however, large canting angles can be induced by weak external magnetic fields.⁴⁰ This is only possible due to the interfilm exchange, which is mediated through a non-magnetic spacer between the magnetic layers,^{41–45} and is therefore much weaker than the exchange typically found in bulk antiferromagnets.³⁸

We start by considering a magnetic multi-layered structure such as that shown in Fig. 1(a). The structure is based

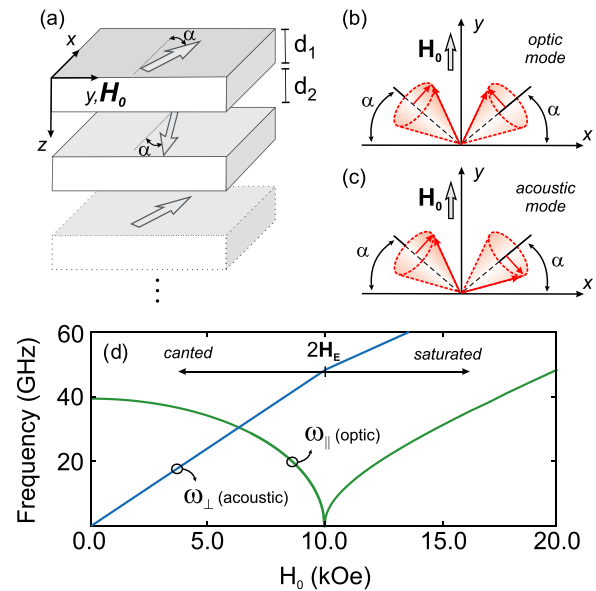


FIG. 1. (a) Geometry of the metamaterial structure composed of alternating magnetic and nonmagnetic layers of thicknesses d_1 and d_2 , respectively. The effect of an externally applied field H_0 along y on the moments (open arrows) creates a canting angle α . (b) Optic and (c) acoustic modes of precession motion of the magnetization in the canted metamaterial. (d) Calculated resonance frequencies of the optic (ω_{\parallel}) and acoustic (ω_{\perp}) modes of a Co/Ru layered metamaterial with both Ru (d_1) and Co (d_2) of 4 Å thickness.

^{a)}Electronic mail: Rair.Macedo@glasgow.ac.uk

on a repetition of two films, one ferromagnetic film of thickness d_1 and a nonmagnetic film of thickness d_2 . The thickness of the nonmagnetic film determines if the coupling between ferromagnetic films is ferromagnetic or antiferromagnetic.³⁵ We are interested in the case of the so-called “anti-phase-domain” configuration, wherein the magnetic ground state in zero external field has the magnetization of a magnetic film aligned antiparallel to that of its nearest neighboring magnetic film⁴⁶ as shown in Fig. 1(a).

This ground state configuration, however, can be perturbed by an externally applied magnetic field H_0 . Here, we consider a static external field applied along y , in which case the moments rotate to partially align with the field direction, as shown in Fig. 1(a). The alignment of the thin film moments can be quantified by an angle α given by^{47,48}

$$\sin \alpha = \frac{H_0}{2H_E}, \quad (1)$$

where H_E represents the interlayer exchange field.

The magnetization in each magnetic film is treated as a macrospin and can precess about its equilibrium direction. The magnetic component of the radiation passing through the metamaterial can couple with these precessions and therefore the radiation can be strongly absorbed near resonances. There are two resonant frequencies for the layered structure shown in Fig. 1(a), belonging to the so-called optic (ω_{\parallel}) and acoustic (ω_{\perp}) modes shown in Figs. 1(b) and 1(c), respectively.^{40,49} The optic mode is particularly important for our application because it has a net dynamic moment along the y axis. These resonance frequencies are shown in Fig. 1(d) for a Co/Ru layered metamaterial with saturation magnetization $M = 17.6/4\pi$ kG, gyromagnetic ratio $\gamma = 2.9$ GHz/kOe, $d_1 = 4$ Å, $d_2 = 4$ Å, and $H_E = 5$ kOe (these values are used throughout this letter unless stated otherwise). Note that the optic mode frequency ω_{\parallel} is quoted in Ref. 40 and can be tuned across a broad range of frequencies using fairly low fields, depending on the strength of the exchange field H_E .

Because we are interested in incorporating this metamaterial within an electromagnetic filter, one must calculate its magnetic permeability tensor. For the structure we are interested in, it can be obtained by a standard thin film effective medium calculation.⁴¹ Here, we simply quote the results of Almeida and Mills^{41,50} that are relevant to our calculation. Using the coordinate system given in Fig. 1(a), the magnetic permeability tensor of the overall layered metamaterial has the same form as that used for hyperbolic natural antiferromagnets,³⁷ and it can be written as

$$\vec{\mu}(\omega) = \begin{bmatrix} \mu_{xx} & 0 & \mu_{xz} \\ 0 & \mu_{yy} & 0 \\ \mu_{zx} & 0 & \mu_{zz} \end{bmatrix}. \quad (2)$$

One of the key criteria for hyperbolic materials is that the sign of one of the diagonal components of the permeability tensor is opposite to that of the other two.⁵¹ Our magnetic multilayer meets this condition as can be seen in Fig. 2(a), where the diagonal components of the permeability tensor are plotted as a function of frequency for the vanishing

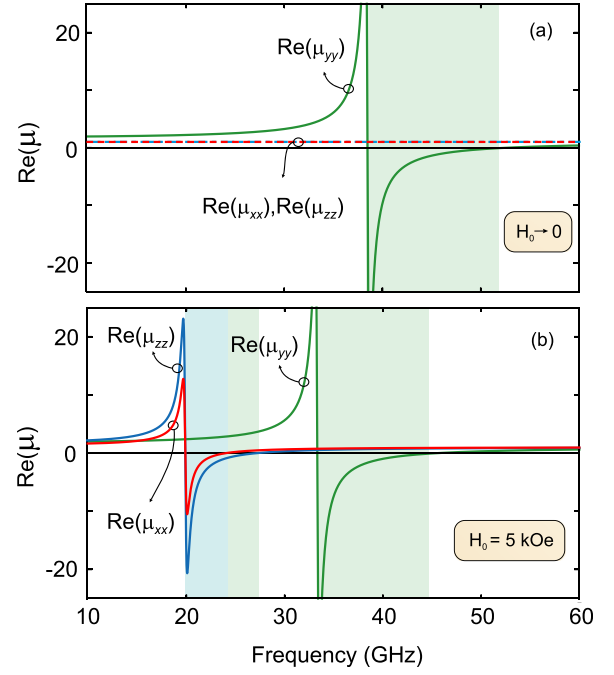


FIG. 2. (a) On-diagonal permeability tensor components as a function of frequency for a Co/Ru layered metamaterial as shown in Fig. 1(a), for the vanishing magnetic field. The shaded region indicates the frequency range over which the material is hyperbolic. (b) The same as panel (a) but showing the effect of an externally applied field $H_0 = 5$ kOe on the permeability tensor components. Here, a phenomenological damping $\Gamma = 0.2$ GHz was used. Green shading represents the frequency range where Type I hyperbolic behavior is found and blue is for Type II.

applied field. In this case, $\mu_{yy} < 0$ for a broad range of frequencies while $\mu_{xx}, \mu_{zz} > 0$ (see the shaded region), which is characteristic of a hyperbolic media of type II.⁵² When an external field is applied and hence spin canting occurs ($\alpha > 0$), the type II hyperbolic behavior associated with μ_{yy} can be tuned to lower frequencies, as illustrated in Fig. 2(b). Note, however, that in the canted spin metamaterial, all components of the permeability tensor now have resonance peaks and not only is another type II region seen ($\mu_{xx}, \mu_{yy} > 0$ and $\mu_{zz} < 0$, green shading) but also a type I hyperbolic region ($\mu_{xx}, \mu_{zz} < 0$ and $\mu_{yy} > 0$, blue shading) can be observed. Thus, we find hyperbolic dispersion at these frequencies, similar to what is observed in conventional hyperbolic media. The hyperbolic isofrequency curves for this metamaterial can be calculated for a given geometry through similar techniques to those employed in natural antiferromagnets.^{34,36}

The general problem of electromagnetic waves propagating in a waveguide containing our material at an arbitrary angle can be quite complicated.²⁴ Here, we concentrate on a simple geometry illustrated in Fig. 3(a), whereby the static applied field along the y axis is perpendicular to the radiation propagation direction along x and is parallel to the dynamic magnetic field \mathbf{h} of the radiation (transverse magnetic or TM mode). (Note that the coordinate axes are the same for Figs. 1 and 3.) In this geometry, the radiation only couples with the μ_{yy} component of the permeability tensor, which has a resonance at the optic mode frequency (the optic mode has a net moment along y). This permeability component is given by^{41,50}

$$\mu_{yy} = 1 + \frac{\gamma^2 16\pi^2 f_1 M^2 \cos^2 \alpha}{\gamma^2 8\pi M H_E \cos^2 \alpha - (\omega + i\Gamma)^2}, \quad (3)$$

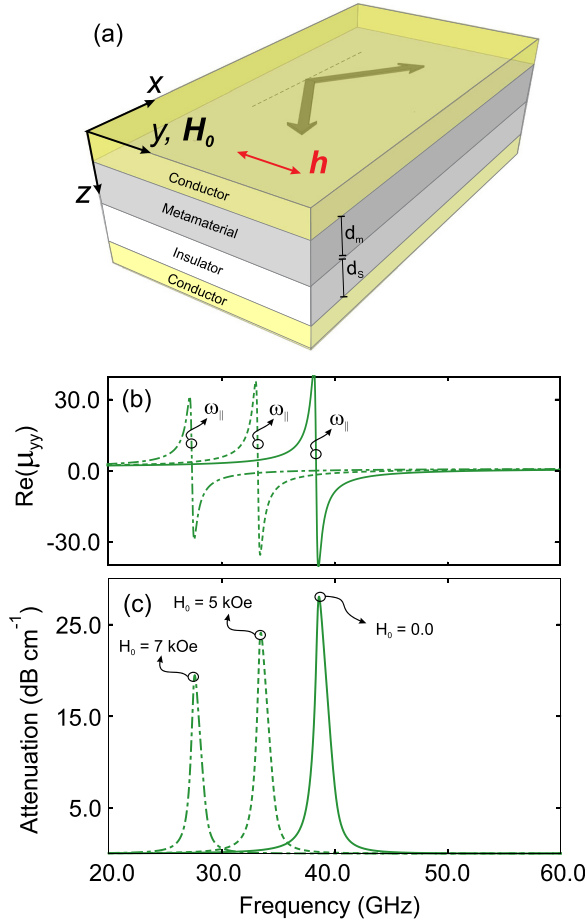


FIG. 3. (a) Geometry of the waveguide structure. A dielectric layer and a metamaterial layer are surrounded by layers of a conducting material. The metamaterial is that shown in Fig. 1(a). The propagation is restricted along x and the externally applied field H_0 lies in the y direction. The incident beam is considered to be TM polarized so that its h field lies in the y direction. (b) $\text{Re}(\mu_{yy})$ and (c) attenuation as a function of frequency for a Co/Ru metamaterial structure, for three values of the static applied field. The thickness of both the Co and Ru layers is 4 \AA . The total thickness of the metamaterial is $d_m = 0.5 \mu\text{m}$ with an assumed conductivity $\sigma = 5 \times 10^6 \text{ S/m}$. The SiO_2 dielectric film has a dielectric constant $\epsilon_2 = 3.9$ and is $5 \mu\text{m}$ thick. Here, a phenomenological damping $\Gamma = 0.2 \text{ GHz}$ was used.

where $f_1 = d_1/(d_1 + d_2)$ is the filling factor for the magnetic material in the multilayer, d_1 is the thickness of the magnetic film, and d_2 is the thickness of the spacer layer. H_E is the effective exchange field, M is the saturation magnetization, and Γ is a phenomenological damping parameter. In Fig. 2(b), we show the behavior of $\text{Re}(\mu_{yy})$ for various externally applied fields, which alter the canting angle α . There are two important frequencies: the resonance frequency ω_{\parallel} and the anti-resonance frequency ω_s which is the frequency where μ_{yy} vanishes. This frequency can be calculated by setting Eq. (3) to zero and isolating ω . In the absence of damping ($\Gamma = 0$), it is given by

$$\omega_s^2 = \gamma^2 \cos^2 \alpha M 8\pi (H_E + 2\pi f_1 M). \quad (4)$$

A solution to Maxwell's equations for this waveguide structure can be found by imposing the required boundary conditions and yields a characteristic equation for the propagation wave vector as a function of frequency given by⁵³

$$k_x^2 = \epsilon_2 \frac{\omega^2}{c^2} + \frac{\epsilon_2 k_{z1}}{d_s \epsilon_1} \tan(d_m k_{z1}), \quad (5)$$

where d_s and d_m are the thicknesses of the insulator substrate and metamaterial, respectively, ϵ_2 is the dielectric constant of the substrate, ϵ_1 is the dielectric constant of the metamaterial given by $\epsilon_1 = 1 + i\sigma/\omega\epsilon_0$ with σ being the conductivity of the magnetic film, and k_{z1} is the wave vector perpendicular to propagation, which is given by

$$k_{z1}^2 = \epsilon_1 \mu_{yy} \frac{\omega^2}{c^2}. \quad (6)$$

The attenuation of the wave per centimeter is proportional to $e^{-\text{Im}(k_x)}$ and is usually quoted in decibels. In Fig. 3(b), we show the behavior of the attenuation as a function of the input TM mode frequency for Co/Ru with filling fraction $f_1 = 0.5$ ($d_1 = 4 \text{ \AA}$ and $d_2 = 4 \text{ \AA}$), for three static applied field values. What is immediately obvious is that there is a narrow absorption band near 40 GHz for vanishing applied field, occurring at the optic mode resonance. The attenuation maximum shifts downward with the increasing field, as expected from Fig. 1(d). The value of the attenuation, 20 dB or larger, is appropriate for integrated devices. The tunability is over 10 GHz for the 7 kOe applied field.

As has been noted earlier, the absorption can be very small near the antiresonance frequency leading to a band-pass like behavior.⁵⁴ In this system, however, the band-pass frequency can be significantly tuned by a very small external field. The tunability is far greater than for the band-stop behavior just discussed. As can be seen in Fig. 4(a), where the real part of μ_{yy} is plotted versus frequency for three values of the static applied field, there is nearly a 30 GHz frequency shift in the antiresonance frequency (the band-pass region) caused by only a 450 Oe magnetic field. This is in

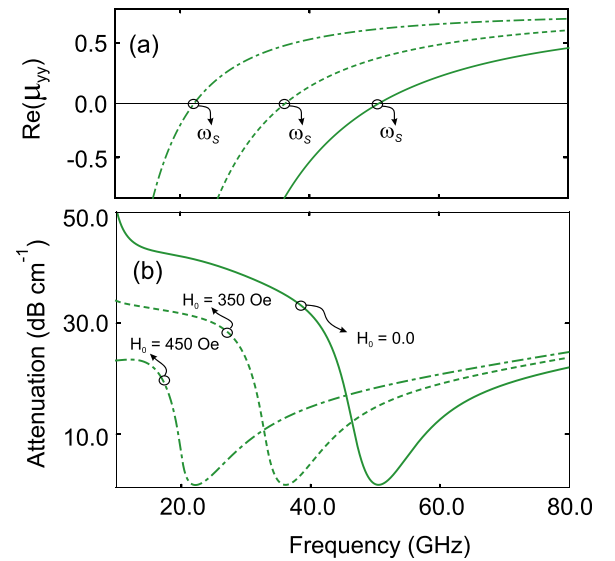


FIG. 4. (a) Real part of μ_{yy} and (b) attenuation as a function of frequency for a Co/Ru metamaterial structure. The parameters for the structure are chosen to give a highly tunable band-pass region. The thickness of the Co layers is 80 \AA , and the Ru layers have a thickness of 4 \AA . The thickness of the metamaterial is $d_m = 5 \mu\text{m}$ with an assumed conductivity $\sigma = 5 \times 10^6 \text{ S/m}$. The dielectric film has $\epsilon_2 = 10$ and is $1 \mu\text{m}$ thick. Here, a phenomenological damping $\Gamma = 0.2 \text{ GHz}$ was used.

stark contrast to what would be obtained for a standard ferromagnet. In that case, the antiresonance frequency is given by $\omega = \gamma(H + 4\pi M)$,⁵⁴ leading to a shift of only 1.5 GHz for a field of 450 Oe. The antiresonance frequency is strongly affected by the filling factor f_1 of the magnetic material in the metamaterial film. By increasing the fraction of the magnetic material, the attenuation peak also increases in frequency. Thus, the band pass region can be designed to operate over a very wide frequency range. Figure 4(b) shows the band pass attenuation for three values of the static magnetic field. Note that in Fig. 4, the filling fraction is $f_1 = 0.95$ ($d_1 = 80 \text{ \AA}$ and $d_2 = 4 \text{ \AA}$), different from that used to make Fig. 3.

In summary, we suggest a type of hyperbolic metamaterial based on a magnetic layered structure. A hyperbolic behavior in the GHz region is realized, in a similar manner to that recently reported for natural antiferromagnetic crystals in the THz region. However, the operating frequencies of the structures suggested here can be tuned using much weaker magnetic fields than those used in natural crystals.³⁷ We have shown how this metamaterial may be used as a band-stop or a band-pass filter, with tunability across tens of GHz on application of a small externally applied field. Only one simple geometry was explored, but other more complicated geometries may lead to richer effects, such as both the acoustic and optic modes being excited by the impinging radiation in the wave guide. Here, we have only used the antiresonance frequency to find minimum absorption, but at this frequency, our metamaterial will also display similar behavior to that found in optical materials with a dielectric constant near zero. These have the unique property that light propagates with almost no phase advance⁵⁵ enabling, for example, electromagnetic flux manipulation⁵⁶ and the emergence of Dirac cones.⁵⁷ While we have concentrated on the application of this structure to microwave filters, we believe that our findings are very relevant in the general context of electromagnetic effects in hyperbolic media, such as guided surface modes, negative refraction,³⁷ and focusing of GHz radiation.³⁴ Note that the conductivity of these structures, modelled here through their dielectric constant, may induce considerable damping. This can influence electromagnetic effects associated with hyperbolic dispersion, depending on the geometry of incidence.

The work of R. Macêdo was financially supported by the Leverhulme Trust, LKAS and SUPA. R. Macêdo would also like to acknowledge the hospitality of The University of Colorado at Colorado Springs, where this work was performed.

¹J. Zhang, J. Zhao, R. Peng, J. Li, R. Zhang, and M. Wang, *Jpn. J. Appl. Phys.* **49**, 033004 (2010).

²J. D. Adam, L. E. Davis, G. F. Dionne, E. F. Schloemann, and S. N. Stitzer, *IEEE Trans. Microwave Theory Tech.* **50**, 721 (2002).

³C. S. Tsai, G. Qiu, H. Gao, L. W. Yang, G. P. Li, and S. A. Nikitov, in *INTERMAG Asia 2005. Digests of the IEEE International Magnetism Conference, 2005* (2005), pp. 1115–1116.

⁴Z. Celinski, I. Harward, N. Anderson, and R. E. Camley, "Magnetism of surfaces, interfaces, and nanoscale materials," in *Handbook of Surface Science*, edited by R. E. Camley, Z. Celinski, and R. L. Stamps (North-Holland, 2015), Chap. 10, Vol. 5, pp. 421–457.

⁵D. Sharma, N. Khare, S. K. Koul, and M. P. Abegaonkar, *Appl. Phys. Lett.* **110**, 182401 (2017).

⁶G. Srinivasan, A. S. Tatarenko, and M. I. Bichurin, *Electron. Lett.* **41**, 596 (2005).

⁷A. S. Tatarenko, G. Srinivasan, and M. I. Bichurin, *Appl. Phys. Lett.* **88**, 183507 (2006).

⁸Y. He, P. He, S. D. Yoon, P. Parimi, F. Rachford, V. Harris, and C. Vittoria, *J. Magn. Magn. Mater.* **313**, 187 (2007).

⁹A. B. Ustinov and B. A. Kalinikos, *Appl. Phys. Lett.* **93**, 102504 (2008).

¹⁰J. Wu, X. Yang, S. Beguhn, J. Lou, and N. X. Sun, *IEEE Trans. Microwave Theory Tech.* **60**, 3959 (2012).

¹¹Y. V. Khivintsev, V. V. Zagorodnii, A. J. Hutchison, R. E. Camley, and Z. J. Celinski, *Appl. Phys. Lett.* **92**, 022512 (2008).

¹²C. Cheng and W. E. Bailey, *Appl. Phys. Lett.* **103**, 242402 (2013).

¹³M. Bao, A. Khitun, Y. Wu, J. Y. Lee, A. P. Jacob, and K. L. Wang, in *2008 Device Research Conference* (2008), pp. 169–170.

¹⁴L. Li, D. Lee, S. X. Wang, M. Mao, T. Schneider, R. Bubber, K. Hwang, and Y. Min, in *INTERMAG 2006—IEEE International Magnetism Conference* (2006), pp. 54–54.

¹⁵M. J. Pechan, C. Yu, R. L. Compton, J. P. Park, and P. A. Crowell, *J. Appl. Phys.* **97**, 10J903 (2005).

¹⁶Y. Zhuang, B. Rejaei, E. Boellaard, A. Vroubel, and J. N. Burghartz, *IEEE Microwave Wireless Compon. Lett.* **12**, 473 (2002).

¹⁷F. Schoenstein, P. Aublanc, H. Pags, S. Queste, V. Barentin, A.-L. Adenot, N. Malljac, and O. Acher, *J. Magn. Magn. Mater.* **292**, 201 (2005).

¹⁸N. Vukadinovic, O. Vacus, M. Labrune, O. Acher, and D. Pain, *Phys. Rev. Lett.* **85**, 2817 (2000).

¹⁹G. Goglio, S. Pignard, A. Radulescu, L. Piroux, I. Huynen, D. Vanhoenacker, and A. Vander Vorst, *Appl. Phys. Lett.* **75**, 1769 (1999).

²⁰Z. Wang, Y.-Y. Song, Y. Sun, J. Bevivino, M. Wu, V. Veerakumar, T. J. Fal, and R. E. Camley, *Appl. Phys. Lett.* **97**, 072509 (2010).

²¹I. Harward, R. E. Camley, and Z. Celinski, *Appl. Phys. Lett.* **105**, 173503 (2014).

²²V. G. Harris, A. Geiler, Y. Chen, S. D. Yoon, M. Wu, A. Yang, Z. Chen, P. He, P. V. Parimi, X. Zuo, C. E. Patton, M. Abe, O. Acher, and C. Vittoria, *J. Magn. Magn. Mater.* **321**, 2035 (2009).

²³Y.-Y. Song, C. L. Ordonez-Romero, and M. Wu, *Appl. Phys. Lett.* **95**, 142506 (2009).

²⁴R. J. Astalos and R. E. Camley, *J. Appl. Phys.* **83**, 3744 (1998).

²⁵B. K. Kuanr, V. Veerakumar, R. Marson, S. R. Mishra, R. E. Camley, and Z. Celinski, *Appl. Phys. Lett.* **94**, 202505 (2009).

²⁶Q. Wang, L. Zeng, M. Lei, and K. Bi, *AIP Adv.* **5**, 077145 (2015).

²⁷K. Bi, W. Zhu, M. Lei, and J. Zhou, *Appl. Phys. Lett.* **106**, 173507 (2015).

²⁸J. S. Zhang, R. L. Zhang, Q. Hu, R. H. Fan, and R. W. Peng, *J. Appl. Phys.* **109**, 07A305 (2011).

²⁹L. P. Carignan, A. Yelon, D. Menard, and C. Caloz, *IEEE Trans. Microwave Theory Tech.* **59**, 2568 (2011).

³⁰A. Encinas, M. Demand, L. Vila, L. Piroux, and I. Huynen, *Appl. Phys. Lett.* **81**, 2032 (2002).

³¹B. Ye, F. Li, D. Cimpoeu, J. Wiley, J.-S. Jung, A. Stancu, and L. Spinu, *J. Magn. Magn. Mater.* **316**, e56 (2007).

³²E. Salahun, P. Quiffec, G. Tann, A.-L. Adenot, and O. Acher, *J. Appl. Phys.* **91**, 5449 (2002).

³³K. H. Kim, M. Yamaguchi, K.-I. Arai, H. Nagura, and S. Ohnuma, *J. Appl. Phys.* **93**, 8002 (2003).

³⁴R. Macêdo, T. Dumelow, and R. L. Stamps, *ACS Photonics* **3**, 1670 (2016).

³⁵J. Fassbender, F. Nörtemann, R. L. Stamps, R. E. Camley, B. Hillebrands, G. Güntherodt, and S. S. P. Parkin, *Phys. Rev. B* **46**, 5810 (1992).

³⁶R. Macêdo, "Tunable hyperbolic media: Magnon-polaritons in canted antiferromagnets," in *Solid State Physics*, edited by R. E. Camley and R. L. Stamps (Academic Press, 2017), Chap. 2, Vol. 68, pp. 91–155.

³⁷R. Macêdo and T. Dumelow, *Phys. Rev. B* **89**, 035135 (2014).

³⁸N. S. Almeida and D. L. Mills, *Phys. Rev. B* **37**, 3400 (1988).

³⁹K. Abrahams and D. R. Tilley, *Infrared Phys. Technol.* **35**, 681 (1994).

⁴⁰R. L. Stamps, *Phys. Rev. B* **49**, 339 (1994).

⁴¹N. S. Almeida and D. L. Mills, *Phys. Rev. B* **38**, 6698 (1988).

⁴²B. Heinrich, Z. Celinski, J. F. Cochran, W. B. Muir, J. Rudd, Q. M. Zhong, A. S. Arrott, K. Myrtle, and J. Kirschner, *Phys. Rev. Lett.* **64**, 673 (1990).

⁴³P. Bruno, *Phys. Rev. B* **52**, 411 (1995).

⁴⁴P. Grünberg, R. Schreiber, Y. Pang, M. B. Brodsky, and H. Sowers, *Phys. Rev. Lett.* **57**, 2442 (1986).

⁴⁵S. S. P. Parkin, *Phys. Rev. Lett.* **67**, 3598 (1991).

- ⁴⁶C. F. Majkrzak, J. W. Cable, J. Kwo, M. Hong, D. B. McWhan, Y. Yafet, J. V. Waszczak, and C. Vettier, *Phys. Rev. Lett.* **56**, 2700 (1986).
- ⁴⁷R. L. Stamps, R. E. Camley, F. C. Nörtemann, and D. R. Tilley, *Phys. Rev. B* **48**, 15740 (1993).
- ⁴⁸F. C. Nörtemann, R. L. Stamps, R. E. Camley, B. Hillebrands, and G. Güntherodt, *Phys. Rev. B* **47**, 3225 (1993).
- ⁴⁹T. Chiba, G. E. W. Bauer, and S. Takahashi, *Phys. Rev. B* **92**, 054407 (2015).
- ⁵⁰Note that our Eq. (3) should correspond to Eq. (3.22) in Ref. 41. However, this equation was later rectified in an Erratum. Our equation is based on the corrected version found at N. S. Almeida and D. L. Mills, *Phys. Rev. B* **39**, 12339 (1989).
- ⁵¹D. R. Smith, W. J. Padilla, D. C. Vier, S. C. Nemat-Nasser, and S. Schultz, *Phys. Rev. Lett.* **84**, 4184 (2000).
- ⁵²A. Poddubny, I. Iorsh, P. Belov, and Y. Kivshar, *Nat. Photonics* **7**, 948 (2013).
- ⁵³V. S. Liao, T. Wong, W. Stacey, A. Ali, and E. Schloemann, in *1991 IEEE MTT-S International Microwave Symposium Digest* (1991), Vol. 3, pp. 957–960.
- ⁵⁴K. L. Livesey and R. E. Camley, *Appl. Phys. Lett.* **96**, 252506 (2010).
- ⁵⁵R. Maas, J. Parsons, N. Engheta, and A. Polman, *Nat. Photonics* **7**, 907–912 (2013).
- ⁵⁶J. Luo, W. Lu, Z. Hang, H. Chen, B. Hou, Y. Lai, and C. T. Chan, *Phys. Rev. Lett.* **112**, 073903 (2014).
- ⁵⁷X. Huang, Y. Lai, Z. H. Hang, H. Zheng, and C. Chan, *Nat Mater.* **10**, 582 (2011).